Perovskite Nanoparticles

DOI: 10.1002/anie.200602571

Template-Free, Low-Temperature Synthesis of Crystalline Barium Titanate Nanoparticles under Bio-Inspired Conditions**

*Richard L. Brutchey and Daniel E. Morse**

Perovskite materials are of interest because they have a wide range of useful applications, for example, in ferroelectric random access memory (FeRAM), piezoelectric transducers, solid-oxide fuel cells, high-temperature superconductors, thermoelectrics, ferromagnets, capacitors, pyroelectric detectors, and colossal magnetoresistors.[1] Perovskites are traditionally prepared by high-temperature solid-state reactions; specifically, $BaTiO_3$ is prepared by the reaction of TiO_2 and $BaCO_3$ at temperatures above 1100 °C, which yields a wide range of grain sizes (0.5–3 μm) and provides very little control over the shape of the particles.[2] Consequently, lower-temperature solution-based synthetic routes (for example, sol–gel and hydrothermal methods) are being explored to better control the nanostructure of the $BaTiO_3$ product. O'Brien et al. first reported the synthesis of $BaTiO_3$ nanoparticles of 6–12 nm by a sol–gel reaction at 100–140 °C, in the presence of oleic acid as a stabilizing agent.[3a] Niederberger et al. described a nonhydrolytic synthesis of 6-nm $BaTiO_3$ nanoparticles at 200–220 °C.[3b] Additionally, Wang et al. recently reported the hydrothermal synthesis of well-defined 17-nm $BaTiO_3$ nanoparticles at 180 °C under highly alkaline conditions.[3c] The low-temperature synthesis of perovskite nanocrystals is inherently difficult; an accurate control over stoichiometry, a close matching of the reaction rates of the precursors, and the identification of specific conditions for crystallization (that is, temperature, pressure, and pH) are all critically important.[4] While several examples of successful controlled syntheses of $BaTiO_3$ nanostructures now exist, they rely on elevated reaction temperatures (> 140 °C) and/or strongly alkaline conditions for crystallization.

Techniques that mimic biomineralization have received much attention because of nature's ability to produce crystalline biominerals with exquisite nanostructures under inherently benign conditions (low temperature, ambient pressure, and near-neutral pH).[5] We recently developed an entirely new low-temperature bio-inspired method for the nanofabrication of metal hydroxides, oxides, and phosphates, which is based on the "re-engineering" of the mechanisms responsible for the enzyme-mediated generation of silica in marine sponges.[6] We have translated the fundamental mechanisms underlying enzyme-mediated biomineralization to an approach wholly controlled by chemical physics, which uses vapor diffusion to establish temporal and vectorial catalyst gradients for the slow growth of nanocrystals at room temperature and ambient pressure. Herein, we report a vapor-diffusion sol–gel route to well-defined crystalline 6-nm $BaTiO_3$ nanoparticles at low temperatures, in the absence of a structure-directing template.

Nanoparticles of $BaTiO_3$ were readily prepared by the kinetically controlled vapor diffusion of $H_2O_{(g)}/HCl_{(g)}$ into a non-aqueous solution of the single-source bimetallic alkoxide $BaTi[OCH_2CH(CH_3)OCH_3]_6$ at 16 °C [Eq. (1)]. Powder X-ray diffraction (XRD) analysis of the as-prepared material revealed that the nanoparticles consist of crystalline $BaTiO_3$ with the cubic perovskite structure (space group $Pm3m$; Figure 1). The thermodynamically stable polymorph of bulk $BaTiO_3$, on the other hand, is the noncentrosymmetric tetragonal phase (space group $P4mm$), which is a room-temperature ferroelectric material.[1] The lattice constant of $a = 4.052(\pm 0.016)$ Å calculated for the nanoparticles is in excellent agreement with the literature value of $a = 4.058$ Å for cubic $BaTiO_3$ (JCPDS no. 75-0215). Crystalline impurities, such as TiO_2 or $BaCO_3$, were not detected by XRD. In situ heating of the nanoparticles to 750 and 1000 °C causes an incremental increase in particle size to 14 and 32 nm, as a result of the coalescence and agglomeration of the nano-

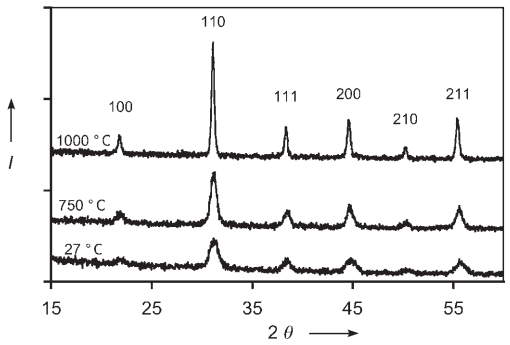

Figure 1. Powder XRD patterns of the $BaTiO_3$ nanoparticles heated in situ to the indicated temperatures.

[*] Dr. R. L. Brutchey, Prof. Dr. D. E. Morse
Institute for Collaborative Biotechnologies
California Nanosystems Institute, Materials Research Laboratory
University of California, Santa Barbara
Santa Barbara, CA 93106-9610 (USA)
Fax: (+1) 805-893-8062
E-mail: d_morse@lifesci.ucsb.edu
Prof. Dr. D. E. Morse
Department of Molecular, Cellular and Developmental Biology
University of California, Santa Barbara
Santa Barbara, CA 93106 (USA)

[**] We thank E. Yoo for his help, as well as Dr. T. Mates and Dr. J. Löfvander for their assistance with the characterization. This work was supported in part by grants from the U.S. Department of Energy (DE-FG03-02ER46006), DARPA (HR0011-04-1-0059), the U.S. Army Research Office (DAAD19-03-D-0004 to the Institute for Collaborative Biotechnologies, and W911NF-05-1-0072), the Biologically Inspired Materials Institute of NASA (NCC-1-02037 and NAG1-01-003), the NOAA National Sea Grant College Program of the U.S. Department of Commerce through the California Sea Grant College System (NA36RG0537, Project R/MP-92), and the MRSEC Program of the National Science Foundation (DMR05-20415 to the UCSB Materials Research Laboratory). The U.S. Government is authorized to reproduce and distribute copies of this Communication for governmental purposes.

Supporting information for this article is available on the WWW under http://www.angewandte.org or from the author.

particles (Figure 1). Similarly, O'Brien et al. obtained 40-nm $BaTiO_3$ nanoparticles after heating 6-nm particles to 700 °C.[3a]

$$BaTi[OCH_2CH(CH_3)OCH_3]_6 + 3\,H_2O_{(g)} \xrightarrow[16\,^\circ C]{HCl_{(g)}\ cat.} BaTiO_3 + 6\,HOCH_2CH(CH_3)OCH_3 \quad (1)$$

Further structural characterization was performed by transmission electron microscopy (TEM). An assembly of quasispherical $BaTiO_3$ nanoparticles, which are partially agglomerated owing to the absence of surface-stabilizing ligands, is shown in Figure 2a,c. The nanoparticles have a

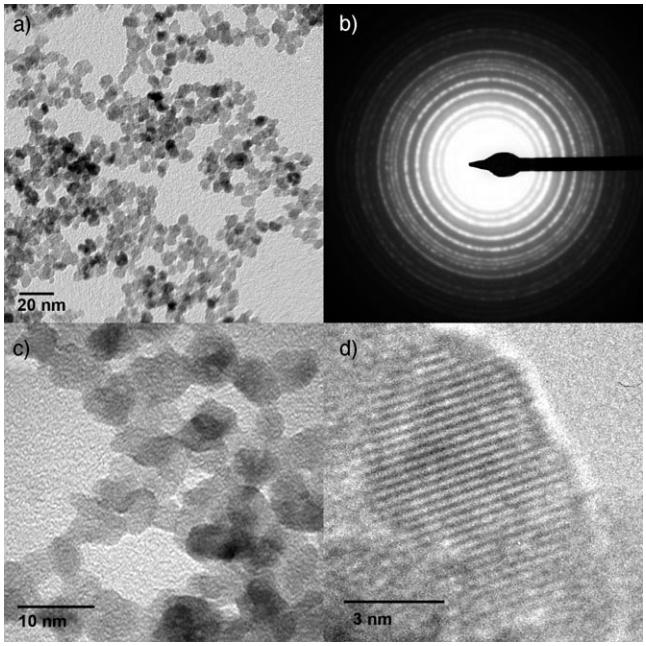

Figure 2. a), c), and d) TEM images of the $BaTiO_3$ nanoparticles at different resolutions. b) SAED pattern of the $BaTiO_3$ nanoparticles.

mean diameter of 5.9 ± 0.1 nm, as measured by TEM, which is in good agreement with the particle size determined by Scherrer analysis of the XRD pattern. A representative selected area electron diffraction (SAED) pattern for the cubic $BaTiO_3$ nanoparticles is presented in Figure 2b. The lattice constant ($a = 4.038(\pm 0.047)$ Å) calculated from randomly selected SAED patterns is in agreement with that determined by XRD. A TEM image of an apparent single-crystalline nanoparticle (oriented along the [110] direction), showing the lattice fringes, is displayed in Figure 2d.

Whereas XRD provides information on long-range order, Raman spectroscopy is a useful technique for probing the structure of the $BaTiO_3$ nanoparticles at the atomic scale, on the basis of vibrational symmetry. Cubic $BaTiO_3$ inherently has no Raman active modes; however, Raman active modes are expected for the noncentrosymmetric tetragonal structure.[7] The spectrum of the as-prepared nanoparticles displays bands at 712 [A_1, E(LO)] and 523 cm^{-1} [E, A_1(TO)], in addition to an intense non-Gaussian band with a maximum at 303 cm^{-1} [B_1, E(TO)], all of which suggest local tetragonal distortion (Figure 3).[7] Even though XRD analysis indicates a cubic perovskite structure, the observed Raman active modes imply a certain degree of tetragonality on the atomic scale.

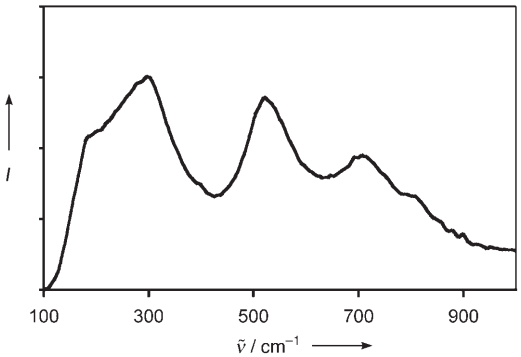

Figure 3. Raman spectrum of the $BaTiO_3$ nanoparticles.

X-ray photoelectron spectroscopy (XPS) was used to confirm the Ba^{2+} and Ti^{4+} oxidation states and coordination environments, as well as to verify the composition of the nanoparticles. The Ba $3d_{5/2}$ and Ti $2p_{3/2}$ binding energies measured for the nanoparticles were 778.3 and 457.8 eV, respectively, which are in excellent agreement with reported values of 778.9 and 458.2 eV.[8] The average surface ratio of Ba:Ti was determined to be 1.3:1, and the XPS spectra did not reveal any contamination by elements other than carbon and chlorine (0.2 wt %). Combustion analysis confirmed a residual carbon content of 3.4 wt %, which presumably results from unhydrolyzed alkoxide ligands. This hypothesis is supported by the observation of Raman bands at 2880 and 2938 cm^{-1} that are indicative of C–H stretches. Moreover, no CO_3^{2-} impurity was detected by Raman spectroscopy.

In bimetallic single-source molecular precursors, two metals A and B are present in a pre-existing geometric relationship. Such precursors have been demonstrated to produce a higher abundance of A–O–B bonds upon conversion to the bimetallic oxide by conventional high-temperature methods (for example, pyrolysis or metal–organic chemical vapor deposition (MOCVD)).[4,9] Utilizing a single-source bimetallic alkoxide in our vapor-diffusion approach yields highly crystalline $BaTiO_3$ nanoparticles at 16 °C, whereas utilizing two separate barium and titanium 2-propoxides as precursors yields an amorphous material under identical conditions. Furthermore, simply adding water (2–100 equiv) to the bimetallic alkoxide yields an amorphous material at 16 °C, a result which is similar to that reported by Hubert-Pfalzgraf et al.[10] Thus, it is the marriage of the single-source bimetallic alkoxide and its temporally controlled catalytic hydrolysis/polycondensation that provides the necessary conditions for the facile crystallization and growth of small, well-defined $BaTiO_3$ nanoparticles at a very low temperature. To our knowledge, similar results have not been achieved to date. Previous syntheses at very low temperatures have produced larger (ca. 50 nm), ill-defined particles.[11]

In summary, we have presented a novel vapor-diffusion sol–gel method that, for the first time, offers a pathway to small, well-defined $BaTiO_3$ nanoparticles at very low temperatures. The synthesis is based on the delivery of water and catalyst in a spatial and temporal gradient to promote the slow, kinetically controlled growth of highly crystalline 6-nm nanoparticles, which are among the smallest reported for $BaTiO_3$. By varying the single-source bimetallic precursor, this methodology may be extended to the synthesis of other perovskite nanoparticles. The ability to rationally synthesize a wide range of technologically interesting perovskite nanoparticles in a controlled manner represents a significant step toward the miniaturization and development of next-generation devices, such as FeRAM.[12]

Experimental Section

All manipulations were performed under an inert atmosphere, and solutions were degassed prior to use. An aqueous solution of HCl (0.75 M, 2 mL) and a separate solution of $BaTi[OCH_2CH(CH_3)OCH_3]_6$ (0.42 M; Gelest, Inc.) in *n*-butanol (0.45 mL) and 2-methoxypropanol (0.75 mL) were placed in an enclosed chamber under argon. The solution containing the bimetallic alkoxide was then exposed to the H_2O/HCl vapor over 15 h at 16 °C to produce the $BaTiO_3$ nanoparticles. The gel product was collected, rinsed with *n*-butanol (3×2 mL), and dried in vacuo. The as-prepared powder was off-white in appearance and could be dispersed in several common organic solvents (for example, THF, hexane, and toluene) with sonication.

XRD was performed on a Bruker D8 Advance X-ray diffractometer with an Anton Parr HTK 16 high-temperature stage, using $Cu_{K\alpha}$ radiation. TEM was done on an FEI Tecnai G^2 Sphera microscope at an operating voltage of 200 kV. SAED patterns were collected at a camera distance of 100 cm for areas selected at random (15 areas on independently prepared samples). The average lattice parameters were determined from the 200 reflection of XRD patterns and from the 320 reflection of SAED patterns. XPS was done on a Kratos Axis Ultra system with a monochromated aluminum anode. The binding energy of C 1s in all spectra was standardized to 285 eV. Raman spectra were obtained on a Nicolet Magna 850 IR/Raman spectrometer. Combustion analyses were performed at the MSI Analytical Lab at UCSB.

Received: June 27, 2006
Published online: September 5, 2006

Keywords: barium titanate · nanostructures · perovskite phases · sol–gel processes

[1] a) M. E. Lines, A. M. Glass, *Principles and Applications of Ferroelectrics and Related Materials*, Clarendon Press, Oxford, **1977**; b) A. S. Bhalla, R. Guo, R. Roy, *Mater. Res. Innovations* **2000**, *4*, 3; c) R. E. Newnham, L. E. Cross, *MRS Bull.* **2005**, *30*, 845.
[2] I. Maclaren, C. B. Ponton, *J. Eur. Ceram. Soc.* **2000**, *20*, 1267.
[3] a) S. O'Brien, L. Brus, C. B. Murray, *J. Am. Chem. Soc.* **2001**, *123*, 12085; b) M. Niederberger, N. Pinna, J. Polleux, M. Antonietti, *Angew. Chem.* **2004**, *116*, 2320; *Angew. Chem. Int. Ed.* **2004**, *43*, 2270; c) X. Wang, J. Zhuang, Q. Peng, Y. Li, *Nature* **2005**, *437*, 121.
[4] K. G. Caulton, L. G. Hubert-Pfalzgraf, *Chem. Rev.* **1990**, *90*, 969.
[5] S. Mann, *Biomineralization Principles and Concepts in Bioinorganic Materials Chemistry*, Oxford University Press, Oxford, **2001**.
[6] a) R. L. Brutchey, E. S. Yoo, D. E. Morse, *J. Am. Chem. Soc.* **2006**, *128*, 10288; b) D. Kisailus, B. Schwenzer, J. Gomm, J. C. Weaver, D. E. Morse, *J. Am. Chem. Soc.* **2006**, *128*, 10276; c) B. Schwenzer, K. M. Roth, J. R. Gomm, M. Murr, D. E. Morse, *J. Mater. Chem.* **2006**, *16*, 401; d) D. E. Morse, *Trends Biotechnol.* **1999**, *17*, 230.
[7] a) M. El Marssi, F. Le Marrec, I. A. Lukyanchuk, M. G. Karkut, *J. Appl. Phys.* **2003**, *94*, 3307; b) G. Busca, G. Ramis, J. M. Gallardo Amores, V. Sanchez Escribano, P. Piaggio, *J. Chem. Soc. Faraday Trans.* **1994**, *90*, 3181.
[8] M. del Carmen Blanco López, G. Fourlaris, B. Rand, F. L. Riley, *J. Am. Ceram. Soc.* **1999**, *82*, 1777.
[9] K. L. Fujdala, R. L. Brutchey, T. D. Tilley in *Topics in Organometallic Chemistry, Vol. 16* (Eds.: C. Copéret, B. Chaudret), Springer, New York, **2005**, pp. 69–116.
[10] L. G. Hubert-Pfalzgraf, S. Daniele, J. M. Decams, J. Vaissermann, *J. Sol-Gel Sci. Technol.* **1997**, *8*, 49.
[11] H. Shimooka, M. Kuwabara, *J. Am. Ceram. Soc.* **1995**, *78*, 2849.
[12] a) R. Waser, A. Rüdiger, *Nat. Mater.* **2004**, *3*, 81; b) N. A. Spaldin, *Science* **2004**, *304*, 1606.

